

Electromagnetic Transition from the 4^+ to 2^+ Resonance in ^8Be Measured via the Radiative Capture in $^4\text{He} + ^4\text{He}$

V. M. Datar,^{1,2} D. R. Chakrabarty,¹ Suresh Kumar,^{1,2} V. Nanal,³ S. Pastore,⁴ R. B. Wiringa,⁵ S. P. Behera,¹ A. Chatterjee,¹ D. Jenkins,⁶ C. J. Lister,⁵ E. T. Mirgule,¹ A. Mitra,¹ R. G. Pillay,³ K. Ramachandran,¹ O. J. Roberts,⁶ P. C. Rout,^{1,2} A. Shrivastava,¹ and P. Sugathan⁷

¹Nuclear Physics Division, Bhabha Atomic Research Centre, Mumbai 400 085, India

²Homi Bhabha National Institute, Anushaktinagar, Mumbai 400 094, India

³Tata Institute of Fundamental Research, Mumbai 400 005, India

⁴Department of Physics and Astronomy, University of South Carolina, Columbia, South Carolina 29208, USA

⁵Physics Division, Argonne National Laboratory, Argonne, Illinois 60439, USA

⁶Department of Physics, University of York, Heslington, York YO10 5DD, United Kingdom

⁷Inter University Accelerator Centre, New Delhi 110064, India

(Received 3 May 2013; published 9 August 2013)

An earlier measurement on the 4^+ to 2^+ radiative transition in ^8Be provided the first electromagnetic signature of its dumbbell-like shape. However, the large uncertainty in the measured cross section does not allow a stringent test of nuclear structure models. This Letter reports a more elaborate and precise measurement for this transition, via the radiative capture in the $^4\text{He} + ^4\text{He}$ reaction, improving the accuracy by about a factor of 3. *Ab initio* calculations of the radiative transition strength with improved three-nucleon forces are also presented. The experimental results are compared with the predictions of the alpha cluster model and *ab initio* calculations.

DOI: [10.1103/PhysRevLett.111.062502](https://doi.org/10.1103/PhysRevLett.111.062502)

PACS numbers: 21.60.De, 23.20.Js, 25.55.-e, 27.20.+n

The nucleus ^8Be is a classic example of the occurrence of alpha clustering [1] in nuclei. Its formation from two alpha particles provides an intermediate step in the synthesis of ^{12}C [2] from the fusion of three alpha particles inside stars. The nucleus is also the stepping stone to understand alpha clustering in heavier self-conjugate $4n$ nuclei. The dumbbell-shaped nucleus exhibits rotational states manifested as resonances in the alpha-alpha scattering system. The electromagnetic transition between the excited resonant states in ^8Be , with spin parities of 4^+ and 2^+ , was reported earlier [3] in order to provide a test for its alpha cluster structure. The radiative capture measurements were made in the $^4\text{He} + ^4\text{He}$ system at two beam energies, on and off the 4^+ resonance. The transition gamma rays were detected in coincidence with the two alpha particles arising from the decay of the 2^+ final state. However, the measured cross section (with an uncertainty of $\sim 33\%$) and the inferred reduced electromagnetic transition rate were not precise enough to provide a stringent test for various models like the cluster model [4] and the *ab initio* quantum Monte Carlo model [5]. The uncertainty arose mainly due to the large background of 4.44 MeV gamma rays originating from the interaction of the incident beam with the window of the chamber holding the helium gas target. This Letter reports a more accurate measurement of the radiative capture cross section at four beam energies straddling the 4^+ resonance and puts the alpha cluster structure of ^8Be on a firmer footing. The essential aspects in this improved measurement are a better pixelization of the alpha particle detectors, a more efficient and

segmented gamma ray detector, and a better shielding of the gamma rays from the beam-window interaction mentioned above.

The experiment was carried out using about 1 pA beams of ^4He from the Pelletron Linac Facility at Mumbai at energies of 19–29 MeV. The schematic of the experimental setup is shown in Fig. 1. The γ rays were detected in a bismuth germanate (BGO) detector array with a photopeak efficiency of about 23% at $E_\gamma = 8$ MeV. The array consisted of 38 hexagonal cross section detectors of length 76 mm and a face-to-face distance of 56 and 58 mm (in two groups). These were close packed into groups of 19 and placed at ~ 70 mm above and below the target. Alpha particles were detected in a 500 μm thick, annular, and double sided silicon strip detector (SiSD), with 2×16 θ rings (in left and right halves) and 16 ϕ sectors [6] with separate readouts. The active portion of the detector had an inner diameter of 48 mm and an outer diameter of 96 mm.

A chamber was designed to mount the strip detector at ~ 70 mm from its center in the forward direction and to hold the target helium gas (purity $>99.9\%$) at ~ 0.8 bar pressure. The gas was isolated from the beam line vacuum using ~ 1 mg/cm² Kapton foils at the entry and the exit. Conical heavymet shields surrounded the Kapton windows in order to shield the BGO detector array from the copious 4.44 MeV γ rays produced in the excitation of ^{12}C in the windows. The chamber had the provision for mounting a thick aluminum aperture plate with a hole of 24 mm diameter as well as thin Mylar and carbon foils. The aperture plate, when placed at the center of the chamber,

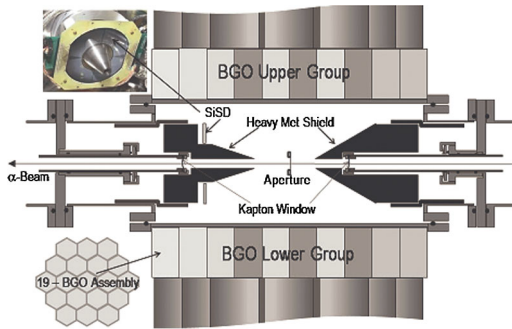


FIG. 1 (color online). Schematic of experimental setup.

shielded the α particles scattered from the Kapton window and limited the effective beam-target interaction zone seen by the SiSD. The aperture diameter and the SiSD distance were decided on the basis of a Monte Carlo simulation [7] to get a reasonable efficiency for the detection of two α particles arising from the decay of the 2^+ final state in ^8Be . The typical effective target length was about 20 mm and the efficiency for the $2\text{-}\alpha$ detection was about 35%.

The energy and timing signals of the SiSD were generated from each of the 32 θ rings (divided into two groups of the left and right halves) and 16 ϕ sectors. The anode signal from the photomultiplier of each of the 38 BGO detectors was used to generate the energy and timing information. The event trigger was generated by requiring a fast coincidence between the left and right halves of the SiSD θ rings and the BGO-detector array. The data were collected in an event-by-event mode using a computer based data acquisition system [8]. A 10 Hz pulser signal was used for estimating the dead time of the data acquisition system.

The energy calibration of the SiSD was done using elastic and inelastic scattering of α particles on ^{12}C and ^{16}O using thin carbon and Mylar targets [9]. The 4.44 and 6.13 MeV γ rays from excited states in ^{12}C and ^{16}O were used to calibrate the BGO detectors. These measurements were made periodically throughout the experiment in order to track the possible change in the calibrations of the α -particle and γ -ray detectors. A stability within $\sim 1\%$ was witnessed over the period of the experiment.

The measurements were made at four beam energies of 19.2, 22.4, 24.7, and 28.9 MeV, spanning the 4^+ resonance in ^8Be , for the integrated beam charges of 81, 90, 125, and 58 μC , respectively. The data were analyzed to extract the events corresponding to the γ -ray transition to the 2^+ final state in ^8Be and its subsequent $2\text{-}\alpha$ decay. The first condition imposed was the prompt coincidence among the γ -ray detector, at least one of the left rings, at least one of the right rings, and two opposite sectors. These conditions emphasize the required events because the two α particles from the decay of the final state are emitted at the azimuthal angles differing by $\sim 180^\circ$, neglecting the small momentum kick due to the transition γ ray. The typical time resolution (FWHM) between the BGO array and the SiSD

was better than 10 ns [10]. The hit multiplicities of the left and the right rings were constrained to one for each and the energy deposited in the left and right halves (E_L and E_R) was constructed from the energy calibrations of the corresponding rings. For getting the γ -ray energy E_γ , the BGO detector with the highest γ -ray energy was taken to be the primary detector. The energies deposited in the neighboring detectors, which were also in prompt coincidence and contained the leaked shower energy, were added to that of the primary detector for each event. An event-by-event reconstruction of the total α -particle energy, $E_{\text{sum}} = E_L + E_R$, was made with conditions of (a) both E_L and E_R being within a lower and an upper limit ($\sim 1\text{--}13$ MeV) and (b) the reconstructed total energy and the total momentum of the two α particles being within an appropriate two-dimensional gate. These conditions were guided by the Monte Carlo simulations described below.

Figure 2 shows a two-dimensional plot of E_{sum} versus E_γ at the beam energy of 22.4 MeV. A band of events around an E_{sum} of 13 MeV and E_γ of 8 MeV can be clearly identified. These events arise from the radiative capture of the two α particles to the 2^+ resonance in ^8Be . A one-dimensional spectrum of $E_{\text{tot}} = E_{\text{sum}} + E_\gamma$ was generated by putting gates on E_{sum} (8.8–15.0 MeV) and on E_γ (3.4–10.5 MeV) as suggested by simulation results. Similar E_{tot} spectra were generated at other beam energies by putting appropriate gates on these quantities. Figure 3 shows the E_{tot} spectra at all four beam energies. The peaks in the spectra (not apparent at the highest beam energy which is beyond the 4^+ resonance), corresponding to the γ -ray transition between the resonances, were used in the calculation of the capture cross sections.

The extraction of radiative capture cross sections requires a simulation of the experimental setup using a Monte Carlo code. The simulation was done in two parts—one for the detection of the two α particles and the other for

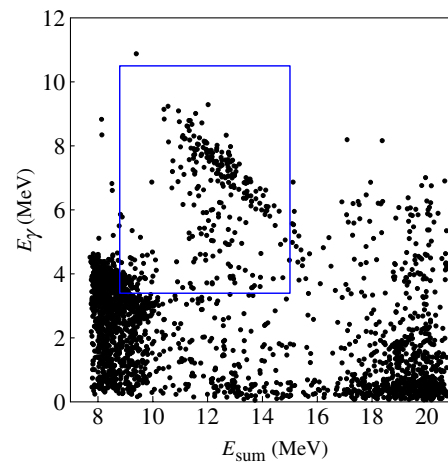


FIG. 2 (color online). Gated two-dimensional spectrum between E_{sum} and E_γ at $E_{\text{beam}} = 22.4$ MeV. The marked events are selected to create the one-dimensional spectrum in Fig. 3.

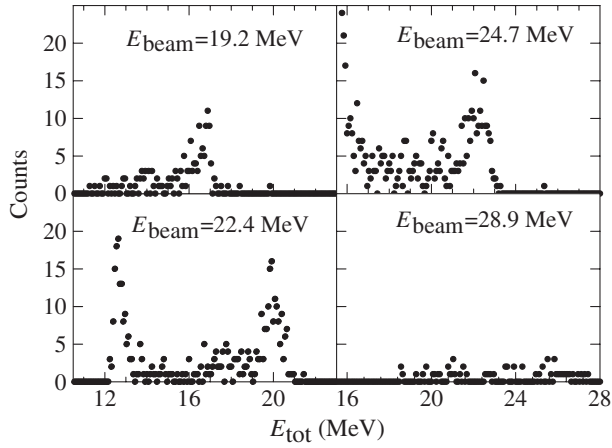


FIG. 3. Gated one-dimensional spectra of E_{tot} at four beam energies.

the response of the BGO array to the incident γ rays. The simulation took into account the extended gas target, the aperture, the angular distribution of the α particles emitted after the γ decay, and the geometry of the SiSD. The energy losses of the beam and decay α particles, and the angular straggling, were calculated for each event using the SRIM code [11]. The γ -ray response was simulated using GEANT3 [12] with the inclusion of angular distribution from the aligned 4^+ to the 2^+ final state. For each event, the γ -ray energy was Doppler corrected. The simulated event-by-event data were written in a file for analysis by the same program that was used to sort the actual data. The simulated data were sorted to create the E_{tot} spectrum with the same conditions as used in the case of the actual data. Starting from the N_0 events corresponding to the 4^+ to 2^+ transition and the subsequent $2-\alpha$ decay, the counts N in the peak regions shown in Fig. 3 were calculated from the simulated spectra to get the overall detection efficiency (N/N_0) of the experimental setup. The capture cross sections were extracted using the detection efficiency, the integrated beam charge, and the effective target thickness provided by the simulation. At each beam energy, the effective α -particle energy E_α was calculated from the knowledge of the interaction region, given by the simulation, and the energy loss of the incident beam in the entrance window and in the target gas up to the interaction region. The spread in E_α due to the finite extent of the interaction region was less than 0.14 MeV. The extracted cross sections at the four E_α values of 18.44, 21.80, 24.08, and 28.40 MeV are 102 ± 12 , 149 ± 16 , 131 ± 13 , and <15 nb, respectively. The cross section at the resonance energy is consistent with the earlier measurement [3], but with an error of $\sim 10\%$ as compared to the earlier 33%.

Figure 4 shows the experimental cross sections along with those calculated by Langanke *et al.* using the alpha cluster model [4]. The contribution from the partial waves of $l = 0, 2, 4$ are added incoherently in this plot. The comparison with experimental data is good in the

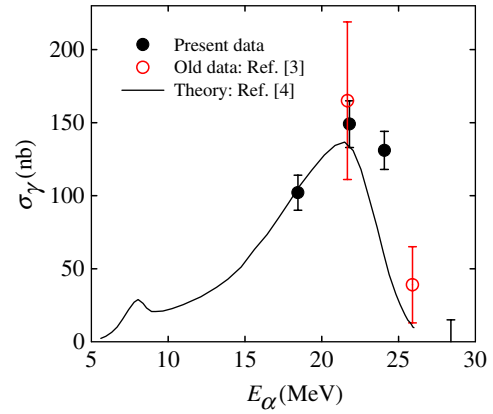


FIG. 4 (color online). Extracted capture cross sections plotted against the effective α -particle energy (see text). The last point indicates the upper bound of the cross section. The continuous line shows the result of a model calculation.

rising part of the cross section profile but deviates at higher energies. Whether a different choice of the α - α potential along with a coherent summing over the various partial waves will improve the comparison remains to be seen. It may be mentioned that there is some ambiguity in the choice of the potentials [13] giving similar values for the energies and widths of the resonant states of ^8Be .

Ab initio calculations of radiative transition strengths in ^8Be , using realistic two- and three-nucleon interactions, were first reported in [5]. These variational Monte Carlo (VMC) calculations of the electric quadrupole moment Q and the reduced transition probability $B(E2)$ indicated that the low-lying spectrum of ^8Be is well described by the rotation of a common deformed $2-\alpha$ structure. Recently, calculations of electroweak transitions have become possible using the more accurate Green's function Monte Carlo (GFMC) method [14]. We report here new GFMC calculations using the Argonne v_{18} two-nucleon [15] and Illinois-7 three-nucleon [16] potentials, which give an excellent reproduction of the spectroscopic properties of $A \leq 9$ nuclei [17].

An initial VMC calculation provides a starting wave function, which the GFMC method then systematically improves upon by a propagation in imaginary time τ . The 2^+ and 4^+ excited states of ^8Be are particularly challenging because they tend to break up into two separate α particles as τ increases. Figure 5 shows the propagation with imaginary time of the energies E , point proton radii r_p , and $E2$ matrix elements. In Fig. 5(a), the $E(\tau)$ drop rapidly from the initial VMC values at $\tau = 0$. The 0^+ ground state energy stabilizes and is well fit by a constant averaged over $\tau = 0.1\text{--}0.3 \text{ MeV}^{-1}$. The 2^+ state shows a small decrease over the same range, while the 4^+ state drifts significantly lower; the energies quoted below are obtained from a linear fit using the value at $\tau = 0.1 \text{ MeV}^{-1}$, with the MC statistical error augmented by

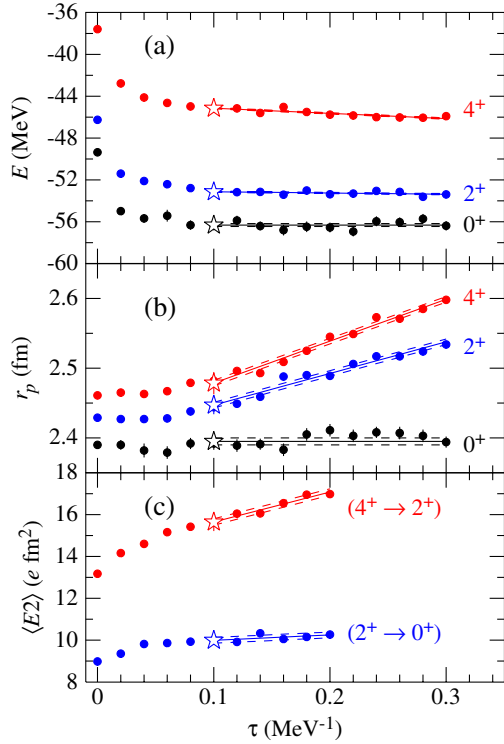


FIG. 5 (color online). GFMC propagation with imaginary time τ of the (a) energy, (b) point proton radius, and (c) $E2$ matrix element. Open stars denote the values extracted from the calculation.

the range of values over $\tau = 0.08\text{--}0.12 \text{ MeV}^{-1}$. This choice of τ should encompass the bulk of the improvement in the wave functions provided by the GFMC algorithm, before the dissolution into two α particles sets in.

This dissolution is seen more strongly in the evolution of r_p shown in Fig. 5(b). The 0^+ ground state radius is flat as a function of τ , while the 2^+ and 4^+ states both increase steadily from about $\tau = 0.1 \text{ MeV}^{-1}$. The Q moments, which are not shown, also increase steadily. Finally, the $E2$ matrix elements, shown in Fig. 5(c), also increase with τ , the effect being particularly pronounced with the ($4^+ \rightarrow 2^+$) transition.

Results for E , r_p , Q , and $B(E2 \downarrow)$ are given in Table I. The energies of the states are in excellent agreement with experiment. The quadrupole moments and $B(E2)$ values are consistent with an intrinsic quadrupole moment Q_0 of $32 \pm 1 \text{ fm}^2$, which is $\sim 20\%$ bigger than the original VMC calculation of Ref. [5].

This result is in contrast to the cluster model [4], which gives a strength for the ($2^+ \rightarrow 0^+$) transition about twice the size of the GFMC calculation. This may be due to their use of structureless α particles. We have evaluated the α - α overlap with the ^8Be states, using the starting VMC wave functions, and obtain spectroscopic factors of 0.84, 0.83, and 0.75 for the 0^+ , 2^+ , and 4^+ states, respectively. If these factors are used, the cluster model cross section would be reduced by a factor of 0.7 and come into better agreement

TABLE I. GFMC results.

J^π	E [MeV]	r_p [fm]	Q [fm^2]	$B(E2 \downarrow)$ [$e^2 \text{fm}^4$]
0^+	-56.3(2)	2.40	0	
2^+	-53.1(1)	2.45(1)	-9.1(2)	20.0(8)
4^+	-45.1(2)	2.48(2)	-12.0(3)	27.2(15)

with the GFMC value. However, the cluster model result for the ($4^+ \rightarrow 2^+$) transition is smaller than the GFMC value even before making such a correction and not as expected for a rigid rotor. Settling this question will require the technically more demanding measurement of the ($2^+ \rightarrow 0^+$) transition.

A comparison with the GFMC calculation needs the present experimental result to be expressed in terms of the $B(E2)$ value for the 4^+ to 2^+ transition. An approximate $B(E2)$ value can be calculated, as in Ref. [4], assuming a Breit-Wigner form factor for the 4^+ resonance. Using the experimental cross section at the resonance energy of $E_\alpha^{\text{cm}} = 10.9 \text{ MeV}$ and an alpha width $\Gamma_\alpha = 3.5 \text{ MeV}$, the extracted gamma width $\Gamma_\gamma = 0.48 \pm 0.05 \text{ eV}$ [18]. Assuming $E(2^+) = 3.04 \text{ MeV}$, the derived $B(E2)$ value is $21 \pm 2.3 e^2 \text{fm}^4$, which is somewhat lower than the calculated value. A better comparison should be possible with the development of true α - α scattering solutions in GFMC calculations, analogous to the case of neutron- α scattering [19], but this is beyond the scope of the present work. The present experimental results will provide data for testing future calculations incorporating the reaction and the structure aspects in a seamless manner.

We thank the Pelletron crew for delivering the ^4He beam and R. Kujur and M. Pose for their help during the experiment. S.P. and R.B.W. wish to thank S.C. Pieper for valuable discussions. The work of C.J.L. and R.B.W. is supported by the U.S. DOE Office of Nuclear Physics under Contract No. DE-AC02-06CH11357; the work of S.P. is supported by the U.S. NSF under Grant No. PHY-1068305.

- [1] A. Bohr and B.R. Mottelson, *Nuclear Structure* (Benjamin, New York, 1975), Vol. 2.
- [2] F. Hoyle, *Astrophys. J. Suppl. Ser.* **1**, 121 (1954).
- [3] V.M. Datar, Suresh Kumar, D.R. Chakrabarty, V. Nanal, E. T. Mirgule, A. Mitra, and H.H. Oza, *Phys. Rev. Lett.* **94**, 122502 (2005).
- [4] K. Langanke and C. Rolfs, *Z. Phys. A* **324**, 307 (1986); *Phys. Rev. C* **33**, 790 (1986).
- [5] R.B. Wiringa, S.C. Pieper, J. Carlson, and V.R. Pandharipande, *Phys. Rev. C* **62**, 014001 (2000).
- [6] Micron Semiconductor Ltd., United Kingdom.
- [7] See Supplemental Material at <http://link.aps.org/supplemental/10.1103/PhysRevLett.111.062502> containing details of the Monte Carlo simulation of the 2-alpha particle detection.

- [8] A. Chatterjee, <http://www.tifr.res.in/~pell/lamps.html>.
- [9] See Supplemental Material at <http://link.aps.org/supplemental/10.1103/PhysRevLett.111.062502> which shows a typical alpha particle spectrum used in the energy calibration of the SiSD detector.
- [10] See Supplemental Material at <http://link.aps.org/supplemental/10.1103/PhysRevLett.111.062502> which shows a typical time spectrum between the SiSD and BGO detectors.
- [11] J. F. Ziegler, <http://www.srim.org>.
- [12] GEANT, version 3.21, CERN program library.
- [13] K. Langanke, *Phys. Lett. B* **174**, 27 (1986).
- [14] M. Pervin, S. C. Pieper, and R. B. Wiringa, *Phys. Rev. C* **76**, 064319 (2007).
- [15] R. B. Wiringa, V. G. J. Stoks, and R. Schiavilla, *Phys. Rev. C* **51**, 38 (1995).
- [16] Steven C. Pieper, *AIP Conf. Proc.* **1011**, 143 (2008).
- [17] S. Pastore, S. C. Pieper, R. Schiavilla, and R. B. Wiringa, *Phys. Rev. C* **87**, 035503 (2013).
- [18] See Supplemental Material at <http://link.aps.org/supplemental/10.1103/PhysRevLett.111.062502> which shows the Breit Wigner fit to the experimental data.
- [19] K. M. Nollett, S. C. Pieper, R. B. Wiringa, J. Carlson, and G. M. Hale, *Phys. Rev. Lett.* **99**, 022502 (2007).